Polar Side Chains Enhance Processability, Electrical Conductivity, and Thermal Stability of a Molecularly p-Doped Polythiophene

Renee Kroon, David Kiefer, Dominik Stegerer, Liyang Yu, Michael Sommer, and Christian Müller**

Molecular doping of organic semiconductors is critical for optimizing a range of optoelectronic devices such as field-effect transistors, solar cells, and thermoelectric generators. However, many dopant:polymer pairs suffer from poor solubility in common organic solvents, which leads to a suboptimal solid-state nanostructure and hence low electrical conductivity. A further drawback is the poor thermal stability through sublimation of the dopant. The use of oligo ethylene glycol side chains is demonstrated to significantly improve the processability of the conjugated polymer p($g_4$2T-T)—a polythiophene—in polar aprotic solvents, which facilitates coprocessing of dopant:polymer pairs from the same solution at room temperature. The use of common molecular dopants such as 2,3,5,6-tetrafluoro-7,7,8,8-tetracyanoquinodimethane (F4TCNQ) and 2,3-dichloro-5,6-dicyano-1,4-benzoquinone (DDQ) is explored. Doping of p($g_4$2T-T) with F4TCNQ results in an electrical conductivity of up to 100 S cm^{-1}. Moreover, the increased compatibility of the polar dopant F4TCNQ with the oligo ethylene glycol functionalized polythiophene results in a high degree of thermal stability at up to 150 °C.

Molecular doping of organic semiconductors is an increasingly explored avenue for optimizing a range of optoelectronic devices. For instance, molecular dopants can be used to improve charge injection through contact doping and to fill traps in field-effect transistors (FETs)[1–3] and organic solar cells.[4–6] In case of organic thermoelectrics molecular dopants permit to increase the charge carrier density (n) and hence tune the performance in terms of electrical conductivity (σ) and Seebeck coefficient (α).[7–9] Another intriguing use of molecular dopants is as a patterning tool by employing the insoluble character of semiconductor:dopant pairs.[10,11]

Deposition of semiconductor and dopant from a single solution is desirable since it minimizes the number of steps needed during processing, which is a key paradigm within the field of organic electronics as it facilitates the use of large-area, high throughput coating, and printing techniques. Coprocessing with p-dopants has been explored for a number of conjugated polymers including polythiophenes such as poly(3-hexylthiophene) (P3HT),[12–20] the bithiophene-thienothiophene copolymer PBTTT,[21,22] polyfluorenes,[23,24] diketopyrolopyrrole-based copolymers,[25,26] and polyaniline.[27] Likewise, coprocessing of n-dopants with the napthalenedicarboximide-bithiophene copolymer P(NDIOD-T2)[28,29] and p-phenylene vinylenes (PPVs)[30–32] has been reported.

For several of these materials, including polythiophenes, such coprocessing leads to inferior results with regard to molecular order of the semiconductor and hence electrical properties. For instance in case of P3HT and 2,3,5,6-tetrafluoro-7,7,8,8-tetracyanoquinodimethane (F4TCNQ), the polymer and dopant form ion pairs, which tend to aggregate.[12,13] Heating of the processing solution dissociates the ion pairs, thereby preventing aggregation, and also enhances the poor solubility of F4TCNQ in commonly used chlorinated processing solvents. However, films cast from hot solution suffer from inferior electrical properties with excess dopant interrupting the nanostructure of the semiconductor. As a result, coprocessed films of P3HT or PBTTT with F4TCNQ tend to display a relatively low electrical conductivity of typically about 0.1–1 S cm^{-1},[14,15,22,33] although in one case, 8 S cm^{-1} was achieved upon addition of as much as 17 mol% of the dopant to P3HT.[20] Moreover, Li et al. found that the poor compatibility of dopant and P3HT leads to poor thermal stability above 90 °C through sublimation of F4TCNQ.[34]

Currently, the most promising approach to circumvent the limitations of coprocessing is sequential doping, where doping is carried out after deposition of the semiconductor through exposure to the dopant dissolved in an orthogonal solvent[20,35–37] or vapor of the dopant by thermal evaporation.[38] The latter method results in an electrical conductivity of up to 5 S cm^{-1} in case of P3HT:F4TCNQ and 250 S cm^{-1} in case of PBTTT:F4TCNQ.[38]

Dr. R. Kroon, D. Kiefer, D. Stegerer, Dr. L. Yu, Dr. C. Müller
Department of Chemistry and Chemical Engineering
Chalmers University of Technology
41296 Göteborg, Sweden
E-mail: renee.kroon@chalmers.se; christian.muller@chalmers.se

D. Stegerer, Dr. M. Sommer
Macromolecular Chemistry
Freiburg University
79104 Freiburg, Germany

DOI: 10.1002/adma.201700930

Synthetic tools that permit to overcome the shortcomings of simultaneous processing of the semiconductor and dopant are less explored. One example was reported by Li et al. who synthesized a series of ester substituted F4TCNQ derivatives, which displayed a higher doping efficiency through improved solubility despite reduced ionization energy (IE).[39] In another study, the same authors investigated doping of an oligo ethylene glycol/sulfonic acid functionalized polythiophene with F4TCNQ, but found a reduced electrical conductivity of not more than 10^{-1} S cm^{-1} despite a stronger semiconductor:dopant interaction, which considerably improved the thermal stability.[34]

We chose to explore doping of a polythiophene that carries polar tetraethylene glycol side chains (denoted p($g_4$2T-T) akin to ref. [40] see **Figure 1**) as opposed to the ubiquitous aliphatic side chains that are generally employed in case of, e.g., P3HT. In addition, this structural alteration causes an increase in the IE of p($g_4$2T-T) as compared to P3HT. Similar polymers with various oligo ethylene glycol side chains were recently used as the anode material in lithium-ion batteries and as the active layer in electrochemical transistors.[40–43] Polar side chains enable the use of more polar solvents such as acetonitrile and dimethylformamide (DMF), which offer better solubility for polar molecular dopants such as F4TCNQ. That is in contrast to less polar (chlorinated) solvents that are commonly used to process alkyl-substituted polymers such as P3HT and PBTTT.

We demonstrate that the use of oligo ethylene glycol side chains is a promising design concept that enables coprocessing of the semiconductor and dopant at room temperature. In addition, the electron-donating ability of ethylene glycol side chains shifts the ionization energy of p($g_4$2T-T), allowing for the use of weaker dopants such as 2,3-dichloro-5,6-dicyano-1,4-benzoquinone (DDQ). As a result, we find a comparable maximum electrical conductivity of up to 100 S cm^{-1} for p($g_4$2T-T) doped with either F4TCNQ and DDQ via solution coprocessing. Moreover, oligo ethylene oxide side chains mitigate sublimation of F4TCNQ. The resulting excellent temperature stability up to 150 °C is of particular interest for the design of organic thermoelectric materials.

The $g_4$2T-T monomer was synthesized according to a modified procedure reported by Song et al.[41] (see Figure 1 and the Supporting Information for experimental details). Stille polycondensation yielded p($g_4$2T-T) with a number-average molecular weight $M_n \approx 16$ kg mol^{-1} (Figure S1, Supporting Information) and an optical bandgap of 1.68 eV (Figure S2, Supporting Information). The polymer could be processed from both chlorinated solvents such as chloroform ($CHCl_3$), dichloromethane, and chlorobenzenes, as well as polar aprotic solvents like tetrahydrofuran (THF), DMF, and acetonitrile (CH_3CN). We found that the stability of p($g_4$2T-T) strongly depends on the choice of solvent. For instance, we observed a rapid blue shift of the UV–vis absorption spectrum in DMF, indicating degradation, whereas in solvents such as chloroform p($g_4$2T-T) appeared stable (Figure S3, Supporting Information). In order to probe aggregation of the polymer, we illuminated p($g_4$2T-T) solutions with a red laser, which resulted in considerable scattering (Figure S4, Supporting Information). We rationalize this observation with the presence of aggregates. Despite this tendency for aggregation, p($g_4$2T-T) offers excellent processability from chlorinated as well as polar aprotic solvents, which we explain with a solvating effect of the polar oligo ethylene glycol side chains that stabilize the polymer against severe coagulation.

In a further set of experiments, we explored coprocessing of p($g_4$2T-T) and the molecular dopant F4TCNQ from solution (**Figure 2**a–c). We chose to compare solutions of (i) 0.2 g L^{-1} p($g_4$2T-T) in a 1:1 mixture of chloroform and acetonitrile (the polymer is processable up to about 20 g L^{-1} at room temperature), with (ii) 0.2 g L^{-1} P3HT in chloroform (note that P3HT is insoluble in 1:1 chloroform:acetonitrile), which appeared blue and yellow, respectively (Figure S5, Supporting Information). Addition of as little as 2 mol% F4TCNQ to P3HT solutions gave rise to noticeable precipitation and a color change,

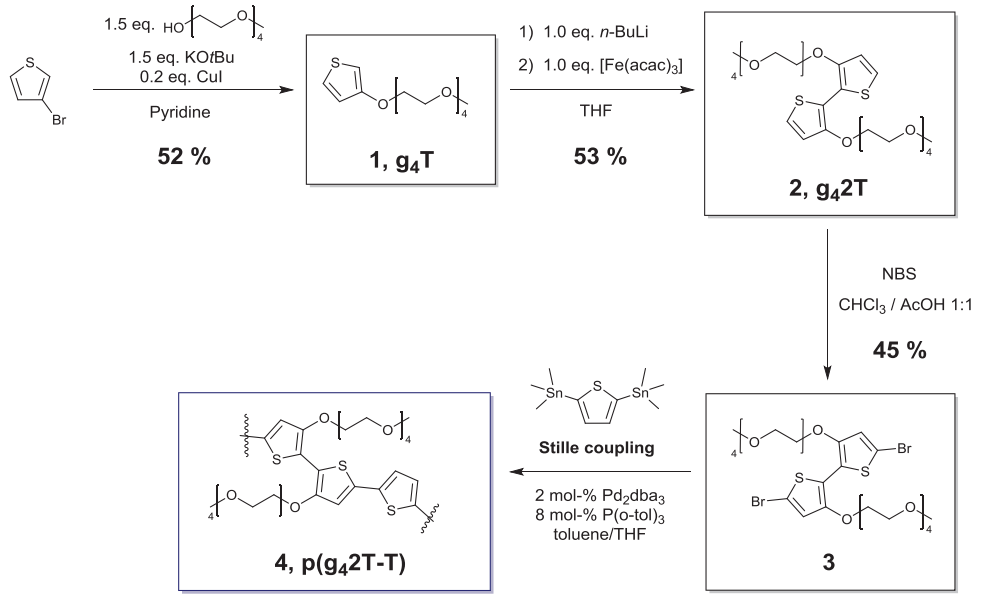

Figure 1. Synthesis scheme of p($g_4$2T-T).

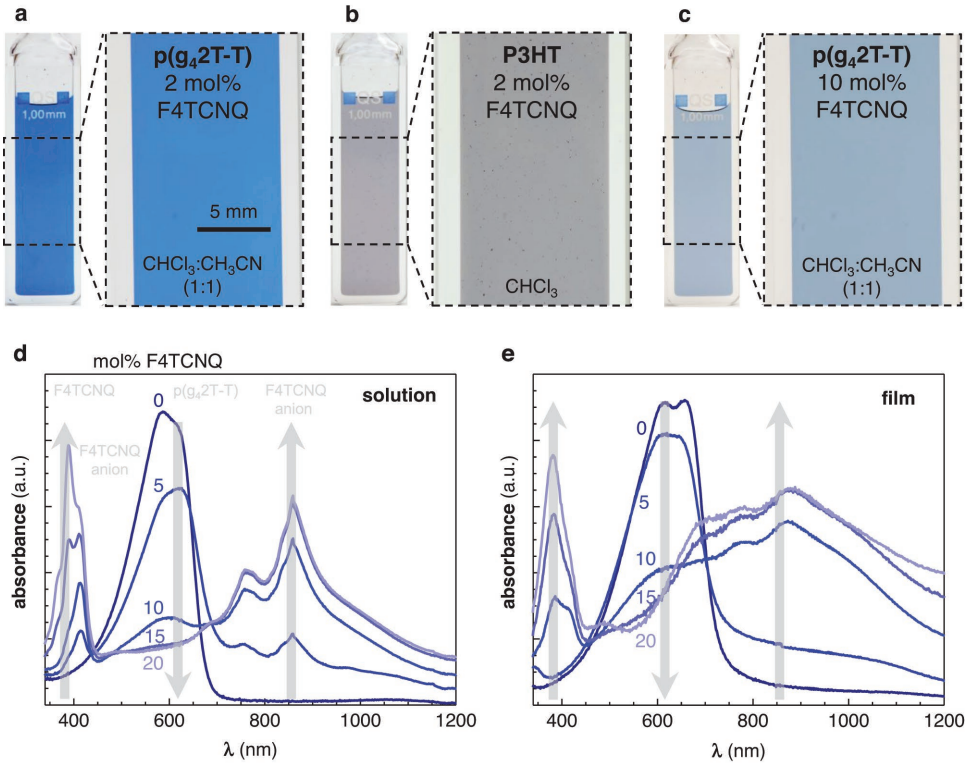

Figure 2. Photographs of p($g_4$2T-T) in 1:1 acetonitrile:chloroform at room temperature, doped with a) 2 mol% and c) 10 mol% F4TCNQ, and b) P3HT in chloroform doped with 2 mol% F4TCNQ. Polymer concentration of 0.2 g L^{-1} was chosen as higher concentrations prevented visible inspection of aggregates. Normalized absorption spectra of d) solutions (1:1 $CHCl_3$:CH_3CN) and e) thin films of pristine p($g_4$2T-T) and doped with 5, 10, 15, and 20 mol% F4TCNQ. Refer to the Supporting Information for full spectra and energy plots.

which is in agreement with previous reports.[20,35] In contrast, addition of up to 5 mol% of F4TCNQ to the p($g_4$2T-T) solution did not result in any visible precipitates or change in color, indicating that the polymer remains solvated. A color change is observed after addition of 10 mol% F4TCNQ to p($g_4$2T-T) but is not accompanied by precipitation. To quantify this result, we performed filtration experiments that show an increase in P3HT residue upon addition of only 2 mol% F4TCNQ, and 78 wt% insoluble material for 5 mol% of the dopant (Table S1, Supporting Information). In contrast, for p($g_4$2T-T) we find a comparable quantity of filtration residue only for 10 mol% F4TCNQ. We would like to note that p($g_4$2T-T) solutions doped with 10 mol% F4TCNQ display mild gelation rather than precipitation, which suggests that coprocessing remains possible even at a higher dopant ratio (Figure 2).

We recorded a series of UV–vis absorption spectra in order to follow doping in solution and the solid state (Figure 2d,e; Figure S6, Supporting Information). We observe several absorption bands whose intensity changes with the doping level: (i) absorption by neat F4TCNQ at 390 nm and F4TCNQ anions at 410 nm,[44] (ii) absorption by neat p($g_4$2T-T) around 600 nm that decreases upon doping, and (iii) sub-bandgap absorption above 700 nm that corresponds to the F4TCNQ anion as well as polarons.[18,33] Solution spectra feature a distinct F4TCNQ anion signal for a dopant fraction of 5 mol% or more, confirming doping already in solution. With increasing dopant concentration the anion absorption increases relative to the absorption of the neat polymer around 600 nm, which disappears for a dopant fraction of 15–20 mol%. Since the absorption around 400 nm originates from both neat dopant and the corresponding anion it is possible to gain information about the absolute abundance of both species by fitting of the spectra within the high-energy region (2.5–3.3 eV). The absorption spectra in this region can be decomposed into (1) a Gaussian representing the contribution from amorphous p($g_4$2T-T), (2) the F4TCNQ anion signal, and (3) the neat F4TCNQ signal (**Figure 3**a; Figure S7, Supporting Information). The extracted intensities of the F4TCNQ anion and the neat F4TCNQ signals were subsequently used to ascertain their concentrations (Figure 3b) and the ionization efficiency (Figure 3c). We find that in solution for up to 5 mol% dopant nearly 100% of F4TCNQ is ionized. Only for dopant molar fractions ≥10 mol% the abundance of neat F4TCNQ increases, while the concentration of F4TCNQ anions stagnates upon further addition of dopant. This observation suggests that about 10 mol% F4TCNQ is needed to fully dope p($g_4$2T-T) in solution. In contrast, a considerable amount of the pristine dopant is present in solid films already at 7.5 mol% F4TCNQ, indicating a reduced degree of doping which we explain with the development of ordered polymer domains.

In order to gain information about the nanostructure of neat and doped films of p($g_4$2T-T), we conducted grazing-incidence wide-angle X-ray scattering (GIWAXS) experiments. As already indicated by differential scanning calorimetry (DSC, Figure S8, Supporting Information), GIWAXS diffractograms confirm the presence of ordered domains in films of neat p($g_4$2T-T) (Figure S9, Supporting Information). Doping of the polymer

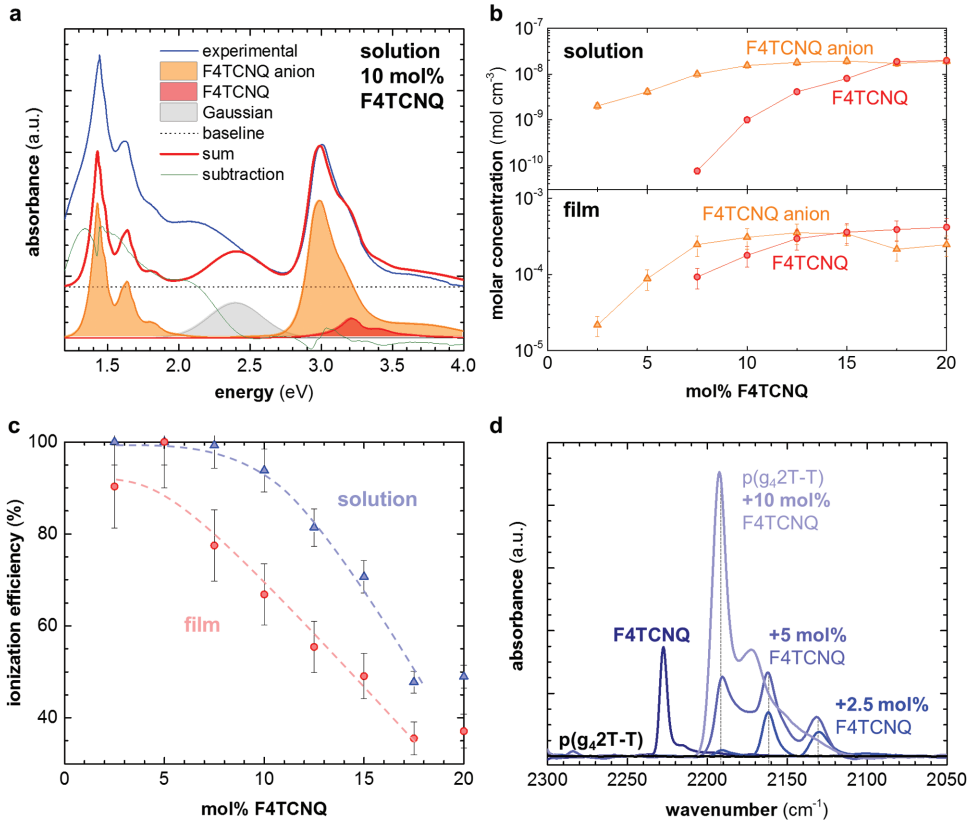

Figure 3. a) Representative optical spectrum of a p($g_4$2T-T) solution doped with 10 mol% F4TCNQ (blue), and decomposition into (1) a Gaussian representing the contribution from p($g_4$2T-T) centered around 2.4 eV, measured absorption spectra of (2) the F4TCNQ anion (orange), and (3) neat F4TCNQ (red). The red curve represents the best fit between 2.5 and 3.3 eV. b) Extracted molar concentrations of F4TCNQ anions (orange) and neat F4TCNQ (red), and c) ionization efficiency in solution and films relative to the F4TCNQ molar fraction (dashed lines are a guide to the eye). d) Fast Fourier transform infrared (FTIR) absorption spectra of solid samples of F4TCNQ, undoped p($g_4$2T-T), and p($g_4$2T-T) doped with 2.5, 5, and 10 mol% F4TCNQ.

with F4TCNQ leads to a shift of the out-of-plane 100 diffraction from 3.6 to 2.9 nm^{-1} as a result of incorporation of the dopant in the polymer crystals, which has also been observed for P3HT doped with F4TCNQ. Interestingly, we do not observe an additional diffraction peak at ≈7.7 nm^{-1} from F4TCNQ crystals (Figure S10, Supporting Information) at higher dopant fractions as has been reported for P3HT:F4TCNQ.[14,45] We argue that the dopant stays molecularly dispersed in the polymer film even after addition of a larger dopant fraction and does not crystallize.

Infrared spectroscopy (IR) was carried out to assess if integer charge transfer occurs between F4TCNQ and p($g_4$2T-T), by recording the cyano stretch vibration of F4TCNQ (Figure 3d). First, a set of IR spectra was recorded of p($g_4$2T-T) with varying amounts of F4TCNQ, in the 2300–2000 cm^{-1} interval. For 2.5 mol% F4TCNQ, three vibrations were observed at 2192 (very weak), 2162, and 2132 cm^{-1}. Then, with increasing F4TCNQ concentration, the cyano stretch vibration at 2192 cm^{-1} increases accordingly. Considering the evolution of the corresponding UV–vis spectra, in particular the appearance of the neutral F4TCNQ peak at 410 nm (Figure 2d) and the absence of the neutral F4TCNQ signal in the 2.5 mol% UV–vis spectrum, the vibration at 2192 cm^{-1} should be attributed to what can be considered the neutral F4TCNQ, i.e., dissolved F4TCNQ in the p($g_4$2T-T) phase (Note that other papers assign this vibration to the F4TCNQ anion, cf. ref. 13). We assign the signal at 2162 and 2132 cm^{-1} to the $F4TCNQ^{-1}$ anions and $F4TCNQ^{-2}$ dianions, respectively. Dianions have been observed previously.[46–48] From the shift in vibrational energy, the degree of charge transfer (δ) can be quantified according to

$$\delta = \frac{2\Delta\upsilon}{\upsilon_0}\left[1-\frac{\upsilon_1^2}{\upsilon_0^2}\right]^{-1} \quad (1)$$

where υ_0 = 2192 cm^{-1} and υ_1 = 2162 cm^{-1} are the wavenumbers recorded for neat (dissolved) F4TCNQ and the anion, respectively, and $\Delta\upsilon = \upsilon_1 - \upsilon_0$. Softening of the cyano stretch vibration of F4TCNQ by $\Delta\upsilon \approx -30$ cm^{-1} is indicative of integer charge transfer ($\delta \approx -1$, note that assignment of the 2227 and 2192 cm^{-1} signals to neat F4TCNQ and its anion, respectively, would also lead to the conclusion that integer charge transfer takes place).[49] To further verify this interpretation, IR spectra were recorded of a freshly prepared solution of F4TCNQ in tetraethylene glycol and the exact same solution after 20 h and compared with their corresponding UV–vis spectra (Figure S11, Supporting Information). The UV–vis spectra of both solutions show a pronounced peak at 352 nm, which we attribute to molecularly dissolved F4TCNQ, as well as the typical anion

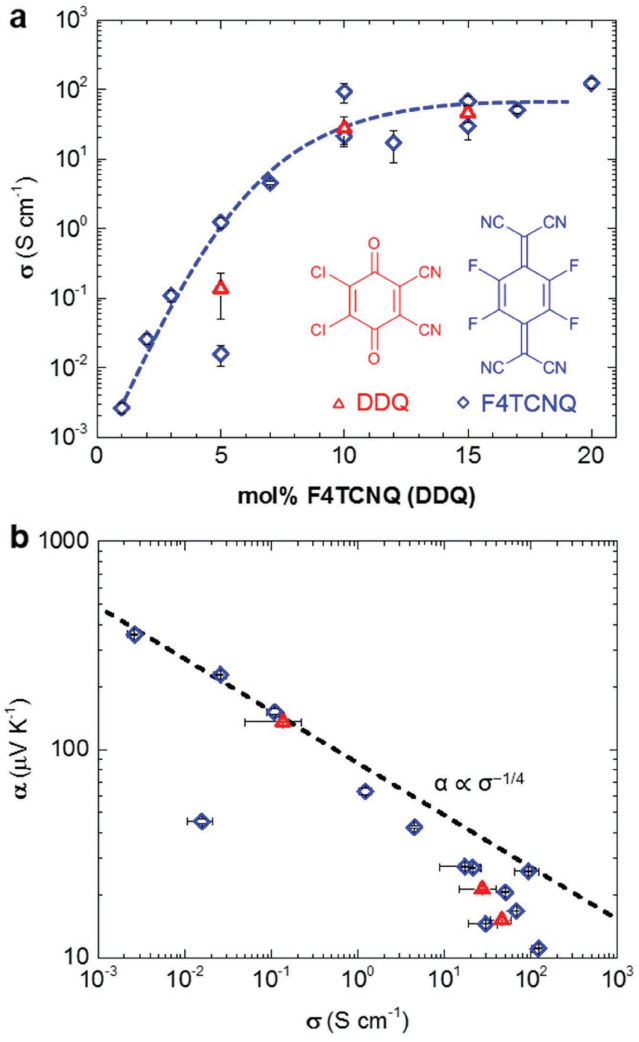

Figure 4. Thermoelectric characteristics of thin films of p($g_4$2T-T) and F4TCNQ (blue) or DDQ (red), processed at room temperature (thickness ≈50–150 nm). a) Electrical conductivity σ as a function of dopant molar fraction (dashed line is a guide to the eye). Molar fractions are calculated with regard to the average molecular weight of one thiophene unit, i.e., $M_{\text{repeat unit}}/3$. b) Seebeck coefficient α as a function of σ in comparison to the empirical correlation $\alpha \propto \sigma^{-1/4}$ proposed by Glaudell et al. (dashed line).[22]

signals at 415, 760, and 864 nm. After 20 h, the intensity of the anion signal has increased relative to the neat F4TCNQ signal in both the UV–vis and IR spectra, strongly suggesting that the cyano stretch vibration at 2162 cm^{-1} is indeed that of the anion. Thus, p($g_4$2T-T) undergoes integer charge transfer with F4TCNQ.

We went on to study the electrical properties of coprocessed p($g_4$2T-T):F4TCNQ thin films (see **Figure 4** for spin-coated films and Figure S12 in the Supporting Information for drop-cast films). In a first regime up to 10 mol% dopant, the electrical conductivity increased by several orders of magnitude from around $\sigma \approx 10^{-5}$ up to 10^2 S cm^{-1}. Instead, for samples containing more than 10 mol% F4TCNQ we observe a similar $\sigma \approx 10^2$ S cm^{-1}. This trend correlates with the relative abundance of neat and anionic F4TCNQ deduced from UV–vis absorption spectra (cf. Figure 3) indicating that about 10 mol% dopant is needed to fully dope p($g_4$2T-T). In case of other polythiophenes such as P3HT, the presence of neat dopant is known to disrupt the nanostructure of the polymer, which negatively affects the charge carrier mobility and hence electrical conductivity.[14,15] Instead, the here studied p($g_4$2T-T):F4TCNQ system appears to be less sensitive to the presence of excess dopant. Glaudell et al. have proposed an empirical correlation between the electrical conductivity and the Seebeck coefficient, i.e., $\alpha \propto \sigma^{-1/4}$, that can be employed to determine whether doped semiconductors are mobility limited by low or nonconducting domains such as excess dopant.[22,33] For coprocessed p($g_4$2T-T):F4TCNQ we find that α continuously decreases with increasing doping level and that a plot of log α versus log σ shows a linear trend with deviations at higher dopant concentrations (Figure 4b). For the here studied system we observe that the amount of F4TCNQ anions levels off above 10 mol% F4TCNQ (cf. Figure 3). Further doping leads to the presence of nonionized F4TCNQ. We propose that this excess dopant fraction increasingly disrupts the nanostructure of the polymer, which to some extent impairs charge transport. As a result, further doping leads to a reduction in Seebeck coefficient but not any significant increase in electrical conductivity (cf. Figure 4). Nevertheless, coprocessed p($g_4$2T-T):F4TCNQ features an electrical conductivity that is up to 15 times higher than coprocessed P3HT:F4TCNQ films, which we attribute to more efficient ion-pair generation between p($g_4$2T-T) and F4TCNQ. This is the result of a decreased IE (cf. IE ≈ 4.4 eV for p($g_3$2T-T)[42] as compared to IE ≈ 4.8 eV for P3HT) through the chemical design of the side chain with an electron-donating oxygen atom directly bound to thiophene, which increases the electron density along the backbone of the neat polymer.

In a further set of experiments we demonstrate that even dopants with a significantly reduced electron affinity (EA) compared to F4TCNQ (EA ≈ 5.2 eV) can be used to efficiently dope p($g_4$2T-T). Coprocessed films of the polymer and the dopant DDQ (EA ≈ 4.6 eV)[39,50] displayed comparable electrical properties as p(g_4 2T-T):F4TCNQ (Figure 4). Hence, the decreased IE of p($g_4$2T-T) opens up the possibility to use dopants that only poorly function with most polythiophenes such as P3HT and PBTTT because of energy level mismatch.

The efficiency and applicability of thermoelectric materials is determined by the temperature difference that can be sustained. Therefore, in a final set of experiments we studied the thermal stability of F4TCNQ-doped p($g_4$2T-T) films, which we compare with doped P3HT (**Figure 5**). We find that the two polymers doped with the same molar fraction of F4TCNQ display very different behavior upon gradual heating to 180 °C. The electrical conductivity of doped P3HT starts to irreversibly decrease already below 100 °C, which we explain with evaporation of F4TCNQ. Instead, doped p($g_4$2T-T) features an almost constant electrical conductivity up to 150 °C (note that thermogravimetric analysis confirms stability of p($g_4$2T-T) in air up to 250 °C; Figure S13, Supporting Information). A second study focused on determining sublimation of F4TCNQ from either a P3HT or p($g_4$2T-T) matrix (Figure S13, Supporting Information). For 10 mol% F4TCNQ in P3HT, we find a sublimation onset of 110 °C and a sublimation rate of $1.4 \cdot 10^{-4}$ mg s^{-1}.

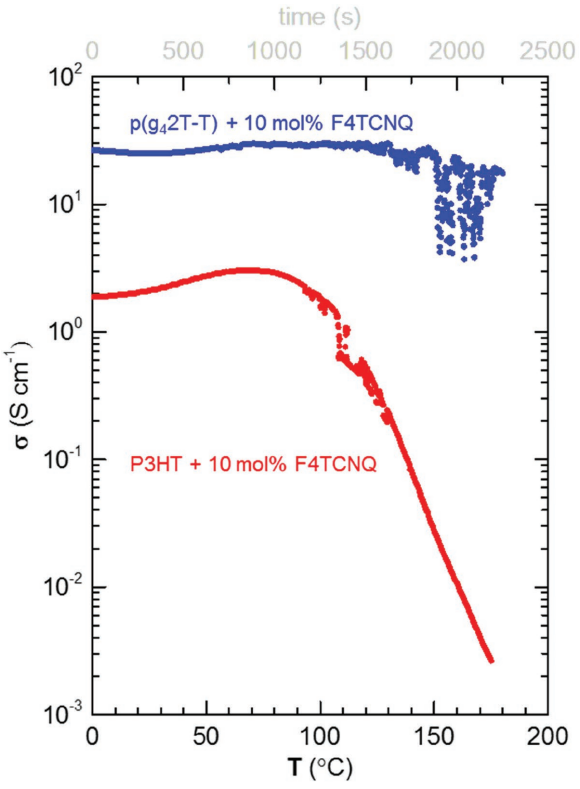

Figure 5. Electrical conductivity of representative drop-cast samples of F4TCNQ-doped p($g_4$2T-T) (blue) and P3HT (red) during heating in air (thickness ≈2 µm). Fluctuations in case of p($g_4$2T-T) are a result of contact problems at elevated temperatures. Note that the pristine polymer features several phase transitions with an onset at 150 °C (Figure S5, Supporting Information). Measurements were limited to a maximum temperature of 180 °C to avoid deformation of poly(ethylene terephthalate) (PET) substrates.

Instead, the sublimation onset is higher and the sublimation rate is more than half for 10 mol% F4TCNQ in p($g_4$2T-T), i.e. 120 °C and 1.4×10^{-4} mg s^{-1}. This observation is in agreement with a study by Li et al. who found a higher thermal stability for an F4TCNQ-doped polythiophene that carried both oligo ethylene glycol side chains and a pendant sulfonic acid group.[34] We rationalize the improved thermal stability with the polar nature of oligo ethylene glycol side chains that improve binding of the molecular dopant F4TCNQ. Moreover, it has been argued that a reduction in the density of side chains increases the space that is available for the counterion, which leads to an improved thermal stability.[51]

In summary, we have shown that the introduction of oligo ethylene glycol side chains strongly assists molecular doping of a polythiophene. The polar side chains enable coprocessing of the polymer with the dopant F4TCNQ or DDQ from solution without the risk for precipitation, which allowed us to prepare thin films with an electrical conductivity of up to 100 S cm^{-1}. Moreover, we have demonstrated that polar side chains considerably improve the thermal stability despite the use of volatile molecular dopants, which is of particular interest for organic thermoelectrics. We argue that polar side chains are a general design principle that can be used to enhance the compatibility of organic semiconductors with molecular dopants.

Supporting Information

Supporting Information is available from the Wiley Online Library or from the author.

Acknowledgements

R.K. and D.K. contributed equally to this work. The financial support from the Swedish Research Council Formas, the Knut and Alice Wallenberg Foundation through a Wallenberg Academy Fellowship, and the European Research Council (ERC) under grant agreement no. 637624 is gratefully acknowledged. The authors thank the Cornell High Energy Synchroton Source (CHESS) (supported by the NSF & NIH/NIGMS via NSF award DMR-1332208) for providing experimental time for GIWAXS measurements.

Keywords

electrical conductivity, molecular dopants, polythiophenes, organic semiconductors

Received: February 15, 2017
Published online: April 24, 2017

[1] G. Lu, J. Blakesley, S. Himmelberger, P. Pingel, J. Frisch, I. Lieberwirth, I. Salzmann, M. Oehzelt, R. Di Pietro, A. Salleo, N. Koch, D. Neher, *Nat. Commun.* **2013**, *4*, 1588.
[2] B. Lüssem, C. M. Keum, D. Kasemann, B. Naab, Z. Bao, K. Leo, *Chem. Rev.* **2016**, *116*, 13714.
[3] S. Rossbauer, C. Müller, T. D. Anthopoulos, *Adv. Funct. Mater.* **2014**, *24*, 7116.
[4] H. Yan, J. G. Manion, M. Yuan, F. P. García de Arquer, G. R. McKeown, S. Beaupré, M. Leclerc, E. H. Sargent, D. S. Seferos, *Adv. Mater.* **2016**, *28*, 6491.
[5] F. Guillain, J. Endres, L. Bourgeois, A. Kahn, L. Vignau, G. Wantz, *ACS Appl. Mater. Interfaces* **2016**, *8*, 9262.
[6] A. Veysel Tunc, A. De Sio, D. Riedel, F. Deschler, E. Da Como, J. Parisi, E. von Hauff, *Org. Electron.* **2012**, *13*, 290.
[7] R. Kroon, D. A. Mengistie, D. Kiefer, J. Hynynen, J. D. Ryan, L. Yu, C. Müller, *Chem. Soc. Rev.* **2016**, *45*, 6147.
[8] O. Bubnova, X. Crispin, *Energy Environ. Sci.* **2012**, *5*, 9345.
[9] B. Russ, A. Glaudell, J. J. Urban, M. L. Chabinyc, R. A. Segalman, *Nat. Rev. Mater.* **2016**, *1*, 16050.
[10] I. E. Jacobs, J. Li, S. L. Burg, D. J. Bilsky, B. T. Rotondo, M. P. Augustine, P. Stroeve, A. J. Moulé, *ACS Nano* **2015**, *9*, 1905.
[11] I. E. Jacobs, E. W. Aasen, D. Nowak, J. Li, W. Morrison, J. D. Roehling, M. P. Augustine, A. J. Moulé, *Adv. Mater.* **2016**, *29*, 1603221.
[12] J. Gao, J. D. Roehling, Y. Li, H. Guo, A. J. Moulé, J. K. Grey, *J. Mater. Chem. C* **2013**, *1*, 5638.
[13] I. Salzmann, G. Heimel, M. Oehzelt, S. Winkler, N. Koch, *Acc. Chem. Res.* **2016**, *49*, 370.
[14] D. T. Duong, C. Wang, E. Antono, M. F. Toney, A. Salleo, *Org. Electron.* **2013**, *14*, 1330.
[15] D. T. Duong, H. Phan, D. Hanifi, P. S. Jo, T. Q. Nguyen, A. Salleo, *Adv. Mater.* **2014**, *26*, 6069.
[16] P. Pingel, D. Neher, *Phys. Rev. B* **2013**, *87*, 115209.
[17] P. Pingel, R. Schwarzl, D. Neher, *Appl. Phys. Lett.* **2012**, *100*, 143303.
[18] C. Wang, D. T. Duong, K. Vandewal, J. Rivnay, A. Salleo, *Phys. Rev. B* **2015**, *91*, 085205.
[19] E. F. Aziz, A. Vollmer, S. Eisebitt, W. Eberhardt, P. Pingel, D. Neher, N. Koch, *Adv. Mater.* **2007**, *19*, 3257.

[20] I. E. Jacobs, E. W. Aasen, J. L. Oliveira, T. N. Fonseca, J. D. Roehling, J. Li, G. Zhang, M. P. Augustine, M. Mascal, A. J. Moulé, *J. Mater. Chem. C* **2016**, *4*, 3454.
[21] J. E. Cochran, M. J. N. Junk, A. M. Glaudell, P. L. Miller, J. S. Cowart, M. F. Toney, C. J. Hawker, B. F. Chmelka, M. L. Chabinyc, *Macromolecules* **2014**, *47*, 6836.
[22] A. M. Glaudell, J. E. Cochran, S. N. Patel, M. L. Chabinyc, *Adv. Energy Mater.* **2015**, *5*, 1401072.
[23] E. Lim, B.-J. Jung, M. Chikamatsu, R. Azumi, Y. Yoshida, K. Yase, L.-M. Do, H.-K. Shim, *J. Mater. Chem.* **2007**, *17*, 1416.
[24] K.-H. Yim, G. L. Whiting, C. E. Murphy, J. J. M. Halls, J. H. Burroughes, R. H. Friend, J.-S. Kim, *Adv. Mater.* **2008**, *20*, 3319.
[25] S. Yoon, J. Cho, H.-K. Lee, S. Park, H. J. Son, D. S. Chung, *Appl. Phys. Lett.* **2015**, *107*, 133302.
[26] Y. Karpov, T. Erdmann, I. Raguzin, M. Al-Hussein, M. Binner, U. Lappan, M. Stamm, K. L. Gerasimov, T. Beryozkina, V. Bakulev, D. V. Anokhin, D. A. Ivanov, F. Günther, S. Gemming, G. Seifert, B. Voit, R. Di Pietro, A. Kiriy, *Adv. Mater.* **2016**, *28*, 6003.
[27] Y. Cao, P. Smith, A. J. Heeger, *Synth. Met.* **1992**, *48*, 91.
[28] Y. Qi, S. K. Mohapatra, S. Bok Kim, S. Barlow, S. R. Marder, A. Kahn, *Appl. Phys. Lett.* **2012**, *100*, 083305.
[29] R. A. Schlitz, F. G. Brunetti, A. M. Glaudell, P. L. Miller, M. A. Brady, C. J. Takacs, C. J. Hawker, M. L. Chabinyc, *Adv. Mater.* **2014**, *26*, 2825.
[30] M. Lu, H. T. Nicolai, G.-J. A. H. Wetzelaer, P. W. M. Blom, *Appl. Phys. Lett.* **2011**, *99*, 173302.
[31] K. Shi, F. Zhang, C. A. Di, T. W. Yan, Y. Zou, X. Zhou, D. Zhu, J. Y. Wang, J. Pei, *J. Am. Chem. Soc.* **2015**, *137*, 6979.
[32] W. Ma, K. Shi, Y. Wu, Z. Y. Lu, H. Y. Liu, J. Y. Wang, J. Pei, *ACS Appl. Mater. Interfaces* **2016**, *8*, 24737.
[33] D. Kiefer, L. Yu, E. Fransson, A. Gómez, D. Primetzhofer, A. Amassian, M. Campoy-Quiles, C. Müller, *Adv. Sci.* **2016**, *4*, 1600203.
[34] J. Li, C. W. Rochester, I. E. Jacobs, E. W. Aasen, S. Friedrich, P. Stroeve, A. J. Moulé, *Org. Electron.* **2016**, *33*, 23.
[35] D. T. Scholes, S. A. Hawks, P. Y. Yee, H. Wu, J. R. Lindemuth, S. H. Tolbert, B. J. Schwartz, *J. Phys. Chem. Lett.* **2015**, *6*, 4786.
[36] S. N. Patel, A. M. Glaudell, D. Kiefer, M. L. Chabinyc, *ACS Macro Lett.* **2016**, *5*, 268.
[37] Q. Zhang, Y. Sun, W. Xu, D. Zhu, *Macromolecules* **2014**, *47*, 609.
[38] K. Kang, S. Watanabe, K. Broch, A. Sepe, A. Brown, I. Nasrallah, M. Nikolka, Z. Fei, M. Heeney, D. Matsumoto, K. Marumoto, H. Tanaka, S. Kuroda, H. Sirringhaus, *Nat. Mater.* **2016**, *15*, 896.
[39] J. Li, G. Zhang, D. M. Holm, I. E. Jacobs, B. Yin, P. Stroeve, M. Mascal, A. J. Moulé, *Chem. Mater.* **2015**, *27*, 5765.
[40] A. Giovannitti, D.-T. Sbircea, S. Inal, C. B. Nielsen, E. Bandiello, D. A. Hanifi, M. Sessolo, G. G. Malliaras, I. McCulloch, J. Rivnay, *Proc. Natl. Acad. Sci. USA* **2016**, *113*, 12017.
[41] C. K. Song, B. J. Eckstein, T. L. Tam, L. Trahey, T. J. Marks, *ACS Appl. Mater. Interfaces* **2014**, *6*, 19347.
[42] C. B. Nielsen, A. Giovannitti, D. T. Sbircea, E. Bandiello, M. R. Niazi, D. A. Hanifi, M. Sessolo, A. Amassian, G. G. Malliaras, J. Rivnay, I. McCulloch, *J. Am. Chem. Soc.* **2016**, *138*, 10252.
[43] A. Giovannitti, C. B. Nielsen, D. T. Sbircea, S. Inal, M. Donahue, M. R. Niazi, D. A. Hanifi, A. Amassian, G. G. Malliaras, J. Rivnay, I. McCulloch, *Nat. Commun.* **2016**, *7*, 13066.
[44] D. A. Dixon, J. C. Calabrese, J. S. Miller, *J. Phys. Chem.* **1989**, *93*, 2284.
[45] F. Deschler, D. Riedel, A. Deák, B. Ecker, E. von Hauff, E. Da Como, *Synth. Met.* **2015**, *199*, 381.
[46] L. Ma, P. Hu, H. Jiang, C. Kloc, H. Sun, C. Soci, A. A. Voityuk, M. E. Michel-Beyerle, G. G. Gurzadyan, *Sci. Rep.* **2016**, *6*, 28510.
[47] H. T. Jonkman, J. Kommandeur, *Chem. Phys. Lett.* **1972**, *15*, 496.
[48] S. Panja, U. Kadhane, J. U. Andersen, A. I. Holm, P. Hvelplund, M. B. Kirketerp, S. B. Nielsen, K. Stochkel, R. N. Compton, J. S. Forster, K. Kilsa, M. B. Nielsen, *J. Chem. Phys.* **2007**, *127*, 124301.
[49] E. Kampar, O. Neilands, *Russ. Chem. Rev.* **1986**, *55*, 334.
[50] DDQ is considerably cheaper than F4TCNQ; as of December 2016 the price per gram of F4TCNQ available from SigmaAldrich was about 2000 times higher than DDQ.
[51] M. R. Andersson, O. Thomas, W. Mammo, M. Svensson, M. Theander, O. Inganäs, *J. Mater. Chem.* **1999**, *9*, 1933.